Structure of ^{65,67}Co studied through the β decay of ^{65,67}Fe and a deep-inelastic reaction

D. Pauwels,* O. Ivanov, N. Bree, J. Büscher, T.E. Cocolios, M. Huyse,
Yu. Kudryavtsev, R. Raabe, M. Sawicka, J. Van de Walle, and P. Van Duppen
Instituut voor Kern- en Stralingsfysica, K.U. Leuven, Celestijnenlaan 200D, B-3001 Leuven, Belgium

A. Korgul
Institute of Experimental Physics, Warsaw University, ul.Hoża 69, 00-681 Warszawa, Poland

I. Stefanescu, A.A. Hecht, N. Hoteling, and A. Wöhr
Department of Chemistry and Biochemistry, University of Maryland, College Park, Maryland 20742, USA and
Physics Division, Argonne National Laboratory, Argonne, Illinois 60439, USA

W.B. Walters
Department of Chemistry and Biochemistry, University of Maryland, College Park, Maryland 20742, USA

R. Broda, B. Fornal, W. Krolas, T. Pawlat, and J. Wrzesinski
Niewodniczanski Institute for Nuclear Physics, Krakow, PL-31342, Poland

M.P. Carpenter, R.V.F. Janssens, T. Lauritsen, D. Seweryniak, and S. Zhu
Physics Division, Argonne National Laboratory, Argonne, Illinois 60439, USA

J.R. Stone
Department of Chemistry and Biochemistry, University of Maryland, College Park, Maryland 20742, USA and
Department of Physics, University of Oxford, OX1 3PU Oxford, United Kingdom

X. Wang
Physics Division, Argonne National Laboratory, Argonne, Illinois 60439, USA and
Department of Physics, University of Notre Dame, Notre Dame, Indiana 46556, USA

(Dated: March 9, 2009)

The neutron-rich isotopes ^{65,67}Fe and ^{65}Co have been produced at the LISOL facility, Louvain-La-Neuve, in the proton-induced fission of ^{238}U. Beams of these isotopes have been extracted with high selectivity by means of resonant laser ionization combined with mass separation. Yrast and near-yrast levels of ^{65}Co have also been populated in the ^{64}Ni+^{238}U reaction at Argonne National Laboratory. The level structure of ^{65}Co could be investigated by combining all the information from both the ^{65}Fe and ^{65}Co β decay and the deep-inelastic reaction. The ^{65}Fe, ^{65}Co and ^{67}Fe decay schemes and the ^{65}Co yrast structure are fully established. The ^{65,67}Co level structures can be interpreted as resulting from the coexistence of core-coupled states with levels based on a low-energy proton-intruder configuration.

PACS numbers: 23.40.-s,23.20.Lv,21.10.-k,27.50.+e

I. INTRODUCTION

The region around $Z = 28$ and $N = 40$ has drawn considerable interest in nuclear-structure research since the observation in ^{68}Ni of a 0^+ level as the first excited state [1] and the high excitation energy of the first excited 2^+ level [2]. Both properties were regarded as strong indications for the double-magic character of ^{68}Ni. However, despite all the additional information that was acquired over the last decade, the specific role of the $N = 40$ subshell closure and the $Z = 28$ closure on the structure of nuclei around ^{68}Ni is not yet understood. Especially the occurrence of single-particle and collective phenomena close to ^{68}Ni deserves further attention. Therefore, this region remains challenging from both an experimental and a theoretical perspective.

Most early studies were aimed at the structure of the more easily produced nickel and copper isotopes using in-beam γ-ray studies [2, 3, 4], β-decay investigations [5, 6, 7, 8, 9], and (d,^{3}He) pickup reactions [10]. Recently, more exotic nuclei with $Z \geq 28$ have provided experimental information providing a more direct connection with single-particle and collective configurations, e.g., g-factor measurements of ^{69m}Cu and ^{67m}Ni [11] and transition probabilities from Coulomb excitation experiments in ^{68}Ni [12, 13] and $^{67-71,73}$Cu [14, 15]. These results provide complementary, but often also unanticipated and crucial insights, such as the admixture of

*Dieter.Pauwels@fys.kuleuven.be

(1p − 1h) excitations across $Z = 28$ in ^{67m}Ni [11], the superfluid character of ^{68}Ni [12] and the collectivity present in ^{69}Cu [15]. While experiments on the nickel and copper isotopes are currently experiencing a new boost, information on the cobalt isotopes around and beyond $N = 40$ remains scarce. On the other hand, the levels of the lighter odd-mass cobalt isotopes up through ^{63}Co appear to be readily described by treating the observed structures as resulting from a single $\pi f_{7/2}$ proton-hole coupled to the adjacent even-even nickel cores [16].

Until recently, the known experimental observables for the heavier cobalt nuclei near ^{68}Ni were isomeric γ decay in ^{66}Co [4], a 189-keV γ transition in ^{67}Co [17] and ground state half-life values determined in $^{66-71,73}$Co β decay [6, 7, 8, 18, 19]. ^{65}Co is the heaviest odd-mass cobalt isotope for which, prior to this work, a level scheme was proposed [20], albeit one that could not be interpreted. The ^{65}Co level scheme presented in the present paper results from a study of ^{65}Fe β decay, as well as of deep-inelastic data that were initially dedicated to the yrast structure of ^{64}Fe [21]. Also, the study of the subsequent ^{65}Co β decay turned out to be crucial to establish the ^{65}Co structure. In previous β-decay work [22], the $(7/2^-)$ ground state of ^{65}Co was reported to directly β feed the $1/2^-$ state at 1274 keV, which remained an unsolved issue. In addition to the ^{65}Fe-^{65}Co decay study presented here, the β decay of ^{67}Fe was studied in the same experimental campaign and revealed a $\pi(1p-2h)$ isomer at 492 keV in ^{67}Co [23]. While in Ref. [23] the isomer was discussed, the present paper is focussing on a detailed description and discussion of the full ^{67}Fe decay scheme.

There are also theoretical issues. Strong monopole interactions [24] are present between the $\pi f_{7/2}$ orbital and the $\nu f_{5/2}$, $\nu g_{9/2}$ and, according to Refs. [25, 26], even the $\nu d_{5/2}$ orbitals. However, the interactions are not precisely known and, moreover, they currently cannot all be included simultaneously in the same valence space. Nevertheless, the first excited levels in copper and nickel isotopes are generally described in fair agreement with experiment by large-scale shell-model calculations [27] using appropriate effective interactions based on the G matrix [28] and modified further with a monopole correction [29]. Experimental spectroscopic-factor values of the first excited $5/2^-$ state in the copper chain determined up to $A = 65$, are, however, significantly larger than the calculated values [27]. This discrepancy illustrates the deficiency in either the interactions used or in the restricted valence space. Unfortunately, even more demanding calculations are required when the $\pi f_{7/2}$ orbital is active; i.e., for cobalt nuclei and other $Z < 28$ nuclei. With the hitherto limited valence space and current realistic interactions, large-scale shell model calculations are not yet available for a consistent description of these nuclei.

The isotopes that are studied in this paper, ^{65,67}Co, provide important information on the effective interactions in the cobalt isotopes adjacent to ^{68}Ni. Consequently, they also form a good testing ground for the potential magic character of the ^{68}Ni core. The isotopes form a bridge between the spherical nickel isotopes and the region of deformation below $Z = 28$ that is observed to set in gradually in excited states of ^{66}Fe [30, 31] and is proposed for the ^{64}Cr ground state [26, 31, 32]. Because the onset of deformation below $Z = 28$ is understood only qualitatively, it is not clear a priori how the cobalt isotopes are behaving, since the deformation mechanism depends critically on the values of the $N = 40$ and $N = 50$ gaps [25]. It is known that the $N = 40$ subshell closure is already weak in ^{68}Ni ($\Delta E = S_{2n}(Z = 28, N = 40) - S_{2n}(Z = 28, N = 42) = 1.71(3)$ MeV) [33] and decreases further in ^{67}Co ($\Delta E = 1.0(6)$ MeV) [34], although the error bar is large in the latter case. Under the influence of the tensor interaction between protons in the $\pi f_{7/2}$ orbital and neutrons in the $\nu f_{5/2}$ and $\nu g_{9/2}$ orbitals [35], the closure is expected to decrease even further for the $N = 40$ isotones with lower Z. The $N = 50$ energy shell gap in ^{78}Ni is not experimentally determined yet, but the systematics of the $N = 50$ isotones with $Z = 31 - 40$ indicate the persistence of this gap towards nickel [36]. Nuclear structure of the cobalt isotopes was until recently known up to $N = 37$ and the structure of all of the nuclei can be interpreted as originating from a $\pi f_{7/2}^{-1}$ proton hole coupled to its adjacent nickel neighbor. Moreover, the dominant low-energy structure of ^{67,69}Ni and $^{68-70}$Cu can be explained as due to a coupling with excited levels of the ^{68}Ni core [37]. It came, therefore, as a surprise that the first excited level in ^{67}Co arises from excitations across $Z = 28$ [23]. The complementarity of the β-decay and deep-inelastic experiments allows to interpret the ^{65}Co structure. Also, a more detailed ^{67}Fe β-decay scheme is presented and will be discussed extensively.

II. EXPERIMENTAL SETUP

A. β decay at LISOL

Short-lived ^{65,67}Fe and ^{65,67}Co isotopes have been produced at the LISOL facility [38, 39] installed at the Cyclotron Research Center (CRC) at Louvain-La-Neuve (Belgium) with the 30-MeV proton-induced fission reaction on ^{238}U. The two 10 mg/cm^2 thin ^{238}U targets were placed inside a gas catcher in order to stop and thermalize the recoiling fission products in an argon buffer gas with 500 mbar pressure. As the fission products, dragged by the argon flow, come close to the exit hole of the gas cell, they are irradiated by two excimer-pumped dye lasers that resonantly ionize the desired element. The ions leaving the cell are transported through a SextuPole Ion Guide (SPIG) [40] to a high-vacuum environment, where they are accelerated over a potential difference of 40 kV. After separation according to their mass-to-charge ratio A/Q, the ions are implanted into a detection tape surrounded by three thin plastic ΔE β detectors and two

TABLE I: List of the different data sets with indication of the mass A, the laser resonance, the cycle (beam ON/beam OFF/number of cycles per tape move), the total data-acquiring time Δt, the production rate P of the listed isotope and the parameters of equation 1, which determine the γ-ray photo-peak efficiency.

Data set	A	Lasers	Cycle	Δt (h)	Isotope	P (at/μC)	C_1	D_1	C_2	D_2
I	65	Fe	2.4s/2.4s/5	49.9	^{65}Fe	1.23(8)	$85(11)\cdot10^{-5}$	$-792(19)\cdot10^{-3}$	800(1000)	2.16(29)
					^{65}Fe^m	1.20(17)				
II	65	Co	2.4s/2.4s/5	28.6	^{65}Co	6.6(16)	$85(11)\cdot10^{-5}$	$-792(19)\cdot10^{-3}$	800(1000)	2.16(29)
III	65	off	2.4s/2.4s/5	4.4	^{65}Co	< 1.1	$85(11)\cdot10^{-5}$	$-792(19)\cdot10^{-3}$	800(1000)	2.16(29)
					^{65}Fe	< 0.05				
					^{65}Fe^m	< 0.05				
IV	67	Fe	1.4s/1.6s/3	9.9	^{67}Fe	1.37(13)	$3.1(4)\cdot10^{-3}$	$-58(25)\cdot10^{-2}$	0	
V	67	off	1.4s/1.6s/3	5.3	^{67}Co+^{67}Co^m	0.40(8)	$3.1(4)\cdot10^{-3}$	$-58(25)\cdot10^{-2}$	0	
					^{67}Fe	< 0.02				
VI	67	Fe	10s/0s/1	53.9	^{67}Fe	0.45(13)	$1.7(2)\cdot10^{-3}$	$-65(2)\cdot10^{-2}$	0	
VII	67	off	10s/0s/1	8.2	^{67}Co^m	0.51(14)	$1.7(2)\cdot10^{-3}$	$-65(2)\cdot10^{-2}$	0	
					^{67}Co	0.25(7)				
					^{67}Fe	< 0.02				

MINIBALL γ-detector clusters [41].

Important features of the detection setup, described in [42], are the MINIBALL's granularity and the data acquisition through digital electronics. The granularity reduces substantially the loss in photo-peak efficiency due to true γ summing. In the data acquisition, all β and γ events get an absolute time stamp by a 40-MHz clock, so that no timing information gets lost. The β-gated γ spectra contain the γ events that occurred in a prompt time window of 350 ns after a β event. To suppress the true summing of β particles with γ rays in the germanium crystals prompt γ events are vetoed if the β event occurred at the same side of the detection setup [43]. The combination of digital electronics and high selectivity by the laser ion source coupled to mass separation offers the possibility to correlate single γ events and/or β-gated γ events with each other up into the seconds time range [42], which turned out to be crucial to disentangle the $A = 67$ decay scheme from iron down to nickel [23].

For half-life determinations, data were acquired in a cycle where, in a first period, the cyclotron beam was on and the mass separator open, followed by a period where the beam was switched off and the separator closed. After a fixed number of such cycles, the implantation tape was moved in order to remove long-lived daughter and contaminant activities. The cycles used are specified in Table I, which also contains production rates at the exit hole of the gas cell as obtained from the observed γ intensities. Despite the high purity of the argon buffer gas (at the ppb-level) and the careful preparation of the gas cell, the production yield is very sensitive to the impurity level of the buffer gas. Due to slightly different conditions, the ^{67}Fe production rate was a factor of 3 higher in data set IV than was the case in data set VI.

The γ-energy and efficiency calibrations were performed by placing standard ^{133}Ba, ^{137}Cs, ^{152}Eu and ^{60}Co sources at the implantation spot of the detection tape as well as by on-line implantation of ^{90}Rb (with intense γ lines up to 3.317 MeV) and of ^{142}Ba isotopes, which were produced in large amounts. The activity could be calculated from the β rate, but at mass $A = 142$ the large production of ^{142}Cs isotopes had to be coped with. Advantage was taken of the large difference in half lives between ^{142}Cs ($T_{1/2} = 1.7$ s) and ^{142}Ba ($T_{1/2} = 10.7$ min) by acquiring data in a 600s/600s/1 implantation-decay cycle and by not considering the implantation period and the first 10 s of the decay period. The latter notation denotes a cycle of 600 s implantation and 600 s decay and the implantation tape is moved after 1 cycle. The γ photo-peak efficiencies ε_γ (in %) were fitted by the function

$$\varepsilon_\gamma = \frac{1}{C_1 E_\gamma^{-D_1} + C_2 E_\gamma^{-D_2}}, \qquad (1)$$

where E_γ denotes the γ energy in units of keV and the parameters C_1, C_2, D_1 and D_2 are given in Table I for the respective data sets. Note that for data sets IV-VII the second term in the denominator, which fits the low-energy behavior, was fixed to 0, since there are no γ transitions with low energy in the ^{67}Fe decay.

B. Deep-inelastic reaction at ANL

Complementary information for the ^{65}Co level structure was extracted from an experiment performed at Argonne National Laboratory. The prime objective of that experiment was to study excited levels in the neutron-rich iron isotopes populated in deep-inelastic reactions of a 430-MeV ^{64}Ni beam with a 55 mg/cm^2 isotopically-enriched ^{238}U target [21, 44]. The uranium target was located in the center of the Gammasphere array [45] consisting of 100 Compton suppressed HPGe detectors. The nickel beam was produced in bunches separated by 82 ns,

but for the deep-inelastic experiment reported here, only one out of five pulses was allowed to hit the Gammasphere target. This resulted in prompt bursts separated by a 410-ns gap within which delayed γ-ray decays emitted by the reaction products could be studied.

Events were recorded on the basis of three-fold or higher-order coincidences. Data were sorted offline into single γ spectra, γ-γ matrices and γ-γ-γ cubes. More details about the sorting procedure are given in Refs. [21, 44]. Four types of coincidence cubes PPP (prompt-prompt-prompt), DDD (delayed-delayed-delayed), PDD (prompt-delayed-delayed) and PPD (prompt-prompt-delayed) were created by selecting different γ-ray times with respect to the prompt beam bursts. The PPP cube was obtained by selecting only the events recorded within $\pm$20 ns of the beam burst. These events correspond to γ rays emitted by excited levels populated directly in the deep-inelastic reaction. The DDD cube was constructed by selecting only the delayed events (but with the three γ rays within a prompt coincidence window of 40 ns) acquired during the beam-off period. These events consist of γ rays emitted by isomeric states (10 ns to 10 μs range) and/or β-delayed transitions. The PDD and PPD cubes were built by combining the prompt and delayed events and were used to identify transitions above or below isomeric levels. An example of the latter is described in Ref. [44].

III. RESULTS

A. ^{65}Co decay to ^{65}Ni

Fig. 1 presents the vetoed, β-gated γ spectra of data set I with the lasers tuned on the iron resonance in black and of data set II with the lasers on the cobalt resonance in red. Using the same cycle, data with the lasers switched off have also been collected (data set III), only showing a line at 511 keV in the vetoed, β-gated γ spectrum. In data set II, significant contaminant lines are observed at 838 and 1223 keV, originating from the β decay of ^{130m}Sb and ^{98}Y, respectively. ^{130m}Sb and the molecule $^{98}YO_2$ are able to reach the detection tape in a doubly-charged state. In Fig. 1, the full circles indicate lines from the ^{65}Fe to ^{65}Co decay, open squares from ^{65}Co to ^{65}Ni and open triangles from contaminant β decay. The observed transitions, count rates and relative intensities in ^{65}Ni from data set II are listed in Table II, while this information for the transitions observed in ^{65}Ni and ^{65}Co from data set I is summarized in Tables III and IV, respectively.

A decay scheme for ^{65}Co was proposed already in earlier β-decay work [22]. Prompt β-γ-γ coincidences (see Table II) confirmed that the 310- and 963-keV transitions are in cascade. Prompt β-γ events coincident with delayed 63-keV γ rays in a 1-150 μs time window after the β event confirmed that the 1210-keV transition feeds an isomeric state with a 63-keV excitation energy. Out of the total 63-keV decays, 22 % of the activity is missed due to the limited time window of 1 to 150 μs for a 69 μs half-life [46] and 75 % due to internal electron conversion. The half-life effect is taken into account for its γ intensity, as shown in the deduced ^{65}Co decay scheme of Fig. 2. The relative intensity of the 63-keV transition, as shown in Table II, also includes the correction for electron conversion, which is necessary to extract the β branching towards the 63-keV level in ^{65}Ni. No coincidence relationships were observed for the lines of 1273 and 1141 keV, confirming their placement as ground-state transitions [22]. From comparing the off-resonant subtracted β activity with the total γ activity a strong ground state feeding of 91.7(8) % was deduced, which is consistent with Ref. [22].

All observed γ transitions following ^{65}Co β decay exhibit the same growing-in and decay behavior. A half-life of 1.00(15) s was deduced for the ^{65}Co ground state from a single-exponential fit of the time-dependent summed intensity of these β-gated γ lines during the beam-off period. This value is slightly smaller, but certainly not significantly different from the previously determined half-life values of 1.14(3) s [22] and 1.25(5) s [47]. The decay behavior of β and γ rays was fitted in the former work, whereas only single β rays were fitted in the latter.

The deduced ^{65}Co decay scheme of Fig. 2 does not contain the previously assigned 340-, 384- and 882-keV transitions [22]. The 340- and 882-keV γ rays follow the β decay of ^{65}Fe, see section III B, while the expected 384-keV peak integral in the β-γ spectrum would be 17(2) as deduced from the γ intensities given in Ref. [22] and the 310-keV peak integral. No 384-keV peak is observed in the spectrum, but this is still consistent within 2σ with Ref. [22], due to the background conditions.

The structure of ^{65}Ni has also been studied in (t_{pol}, d) transfer reaction experiments [48] from which spin and parities have been deduced for various levels. The $5/2^-$

TABLE II: Transitions in ^{65}Ni from ^{65}Co β decay (data set II) are indicated by their energy E (keV), the corresponding off-resonant subtracted β-gated peak count rate A_γ and transition intensity I_{rel} relative to the 1141.1-keV transition (100 %). Multiply I_{rel} by 0.027 (7) to get absolute intensities. The γ-ray energies of coincident events are listed in the last column with the number of observed β-γ-γ coincidences between brackets.

E (keV)	A_γ (cts/h)	I_{rel} (%)	Coincident γ-events
63.4 (4)	0.9 (2)	65 (18)[a]	1210(3)
310.4 (1)	9.2 (7)	82 (11)	963(16)
963.4 (2)	3.7 (5)	79 (13)	310(16)
1141.1 (2)	4.2 (4)	100	-
1210.6 (2)	1.5 (3)	39 (9)	63(3)
1273.2 (3)	1.6 (3)	42 (9)	-

[a]The relative intensity also includes the correction for electron conversion.

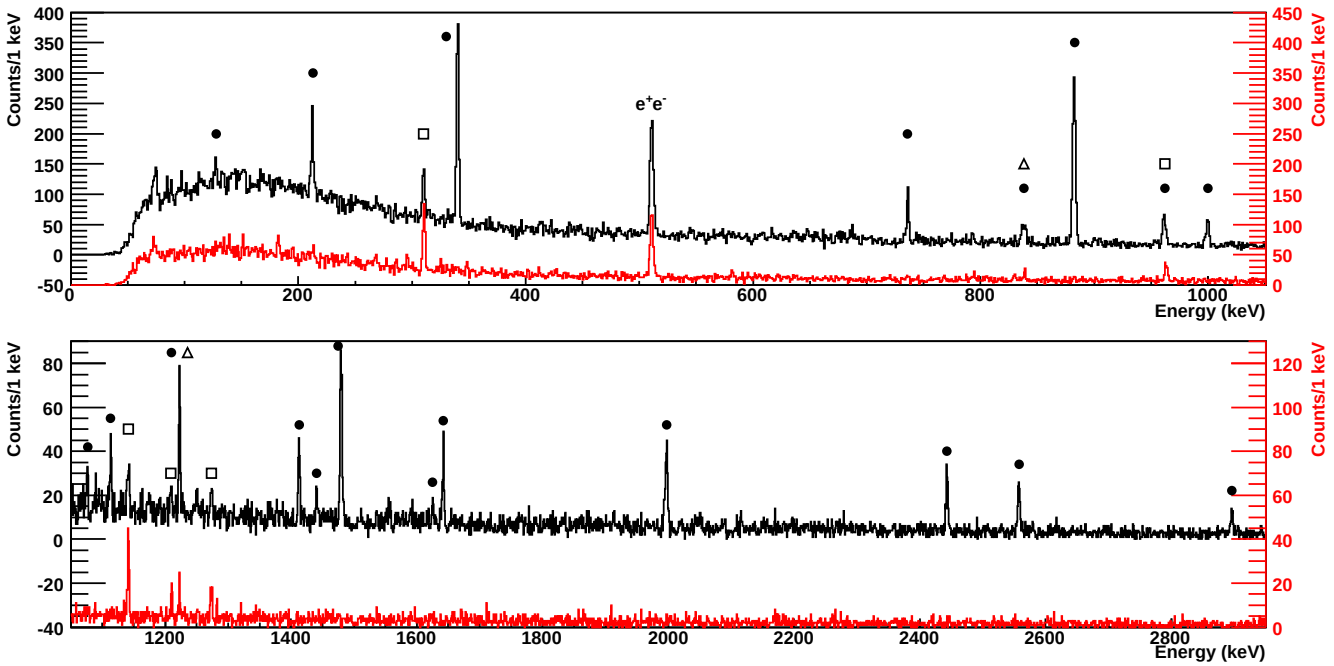

FIG. 1: (Color on-line) The vetoed β-gated γ spectrum with the lasers tuned to ionize iron and cobalt in black and red, respectively. The lines from ^{65}Fe to ^{65}Co decay are indicated by full circles, those from ^{65}Co to ^{65}Ni decay by open squares and contaminant lines by open triangles. Three doublets are present: at 837 (of ^{65}Fe and ^{130m}Sb decay), 962 (of ^{65}Fe and ^{65}Co decay) and 1223 keV (of ^{65}Fe and ^{98}Y decay). The ^{130m}Sb ions and $^{98}YO_2$ molecules were able to reach the detection tape in a doubly-charged form (see text for details).

ground state is strongly fed by direct Gamow-Teller β decay, which is consistent with an expected $(7/2^-)$ ground state of ^{65}Co. The 1141-keV level, for which spin and parity quantum numbers were not yet assigned, is strongly fed. Based on a $(7/2^-)$ ^{65}Co ground state and a lack of γ deexcitation to the low-spin states, a spin and parity of $(7/2^-)$ or $(9/2^-)$ can be expected. Also, the state at 1274 keV gets significant β feeding ($\log ft = 5.1(1)$), and a subsequent strong γ decay is observed to the $5/2^-$ ground state, the $1/2^-$ state at 63 keV and the $3/2^-$ state at 310 keV. The observed γ decay to the 63-keV, $1/2^-$ state rules out $(7/2^-)$ and $(9/2^-)$ assignments and leaves $(5/2^-)$ as the only possibility. This is, however, in disagreement with the previously assigned spin and parity of $1/2^-$ in Ref. [48].

TABLE III: Transitions in ^{65}Ni following ^{65}Fe mother-daughter β decay (data set I) are indicated by their energy E (keV), the corresponding off-resonant subtracted peak count rate A_γ, transition intensity I_{rel} relative to the 882.5-keV transition (100 %) and the ratio of relative transition intensities $\frac{I_{rel}(II)}{I_{rel}(I)}$ from data set II and I.

E (keV)	A_γ (cts/h)	I_{rel} (%)	$\frac{I_{rel}(II)}{I_{rel}(I)}$
63.4 (4)	0.50 (12)	10 (3)	6 (2)
310.4 (1)	4.1 (5)	10.9 (14)	8 (2)
963.4 (2)	1.9 (5)	12 (3)	7 (2)
1141.1 (2)	1.4 (4)	12 (2)	8 (2)
1210.6 (2)	1.0 (5)	8 (2)	5 (2)
1273.2 (3)	1.0 (4)	8 (2)	6 (2)

Missing γ-ray activity from higher lying states feeding the 1274-keV level seems unlikely due to the relatively small β-endpoint energy of 5.956(13) MeV. Furthermore, the $1/2^-$ assignment is not consistent with ^{64}Ni(n,γ) studies. This reaction populates a $1/2^+$ level in ^{65}Ni at 6098 keV [49], which decays predominantly by high-energy $E1$ transitions to $1/2^-$ and $3/2^-$ levels. The (n,γ) work clearly establishes four $1/2^-$ and $3/2^-$ states at low energy (at 64, 310, 692 and 1418 keV). None of these levels are fed directly in the ^{65}Co β decay. Moreover, the 6098-keV level does not populate directly the $5/2^-$ ground state nor the 1141- and 1274-keV states, which indicates that the latter two states have spin $J = 5/2$ or greater. In the event that a $1/2^-$ assignment to the 1274-keV level would have been correct, the strong β feeding would have to originate from a low-spin, β-decaying isomer in ^{65}Co. Penning-trap mass measurements, however, could not identify a β-decaying isomer in ^{65}Co [50].

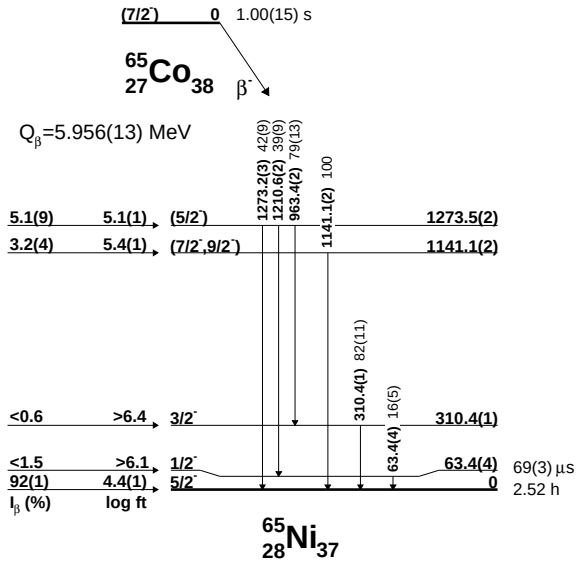

FIG. 2: The ^{65}Co decay scheme into ^{65}Ni. Spin and parities without brackets are taken from [48], while those within brackets are deduced from the present β-decay study.

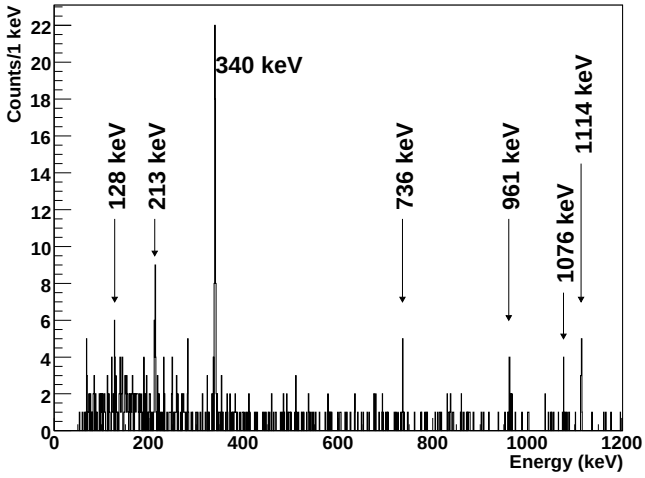

FIG. 3: The γ-ray spectrum of prompt coincidence events with β-gated, 883-keV events (data set I).

B. Level structure in ^{65}Co

1. β-decay study of ^{65}Fe at LISOL

Peaks enhanced in the data with the lasers tuned to the iron resonance and absent in the data with the lasers on the cobalt resonance, can be unambiguously assigned to the ^{65}Fe β decay feeding excited states in ^{65}Co. Hence, the data provide clear evidence that the intense lines at 340 and 883 keV, previously assigned to the ^{65}Co decay [22], occur in fact in the ^{65}Fe β decay. At 838 and 1223 keV, the contaminant activity from the doubly-charged ^{130m}Sb ions and $^{98}YO_2$ molecular ions form a doublet with the iron lines. The relative γ intensities of the iron lines were obtained by subtraction of the off-resonant contribution, which could be deduced from data set II. The iron line at 961 keV also forms a doublet with the 963-keV transition from ^{65}Co decay. Hence, the contribution of the cobalt line is obtained from the 310-keV peak integral and the relative γ intensities of the 310- and 963-keV γ rays, as deduced in the ^{65}Co decay, see Table II. It was checked that the γ intensities of both the 1211-keV and the 1273-keV transitions relative to the 310-keV line in data sets I and II are in agreement.

Two independent level schemes can be constructed using the transitions and their coincidence relations given in Table IV. Starting with the most intense line in Table IV, the 883-keV transition, a level at 883 keV is deduced. Fig. 3 shows the γ spectrum of prompt coincidence events with β-gated, 883-keV events. It reveals a strong coincidence with 340-keV γ rays. In combination with the 1223-keV cross-over transition, the 1223-keV level could be established as shown on the left hand side in Fig. 4. The coincident events at 128 and 213 keV match perfectly the energy difference of 340 keV. Due to its higher intensity, the 213-keV transition is placed below the 128-keV one and on top of the 883-keV γ ray, establishing the 1095-keV level. The 1959-keV state could be established on the basis of the observed coincidences with 1076- and 736-keV events, which differ by 340 keV. The 1076-keV transition is thus placed on top of the 883-keV level and the 736-keV γ line on top of the 1223-keV state. The 864-keV transition towards the 1095-keV level was only observed from coincidences with 213-keV events (and one 883-keV event), see Table IV. The coincidence relationships between 1114- and 883-keV events and a non-coincident cross-over 1997-keV line provide evidence for a 1996-keV state. The 774-keV transition towards the 1223-keV level is only observed from coincidences with 340-, 883- and 1223-keV events, see Table IV. Based on the 961-keV coincidences with 340- and 883-keV events and coincidences between the 1089- and 213-keV events, a level at 2183-keV could be established, from which the 961- and the 1089-keV transitions feed the 1223-keV and 1095-keV states, respectively. The 961-keV coincidences with 310-keV γ rays are due to the 963-keV ^{65}Ni component in this doublet. Based on all the arguments given above, the β-decay scheme is constructed as given on the left in Fig. 4.

The β-decay scheme shown on the right of Fig. 4 is constructed following the same principles. The strongest transitions in this level scheme are the 1480- and 1642-keV transitions feeding the ground state. The 2479-keV level could be established from the 1480- and 1642-keV coincidence relations with 1000- and 837-keV γ rays, respectively. The 2892-keV state could be established on the basis of coincidences between 1413- and 1480-keV events and observed 1000-keV coincidences with 413-keV events. The γ-ray transitions at 1441, 1626, 2443, 2558

TABLE IV: Transitions in ^{65}Co from ^{65}Fe β decay (data set I) are indicated by their energy E (keV), the corresponding off resonant subtracted peak count rate A_γ and transition intensity I_{rel} relative to the 882.5-keV transition (100 %). Multiply I_{rel} by 0.20 (6) to get absolute intensities. The γ-ray energies of coincident events are listed in the last column with the number of observed β-γ-γ coincidences between brackets.

E (keV)	A_γ (cts/h)	I_{rel} (%)	Coincident γ-events
127.6 (3)	1.7 (6)	3.4 (12)	213(8), 736(5), 883(5), 961(2)
212.5 (2)	5.2 (6)	11.1 (13)	128(7), 736(3), 883(17), 1089(7)
340.07 (6)	16.5 (7)	47 (2)	736(27), 774(6), 883(53), 961(8)
413.0 (10)	-	2.6 (12)	1000(4)
736.1 (10)	4.3 (4)	22 (2)	340(28), 883(8), 1223(7)
774.0 (10)	-	6 (4)	340(5), 883(2), 1223(1)
836.6 (2)	2.6 (5)	14 (3)	1642(4)
864.0 (10)	-	1.8 (10)	213(6), 883(1)
882.50 (9)	17.0 (6)	100	128(7), 213(20), 340(53), 736(6), 961(9), 1076(5), 1114(12)
960.5 (2)	1.4 (5)	9 (3)	310(6), 340(10), 883(8)
999.7 (3)	2.7 (4)	18 (2)	413(4), 1480(4)
1076.2 (3)	1.2 (3)	8.3 (18)	883(6)
1088.7 (6)	0.6 (2)	3.9 (13)	213(6), 883(2)
1113.5 (3)	2.1 (3)	15 (2)	883(12)
1222.7 (2)	3.1 (4)	23 (3)	736(7), 774(1), 961(1)
1412.5 (2)	2.6 (3)	22 (3)	1480(7)
1441.1 (4)	0.9 (3)	8 (2)	-
1479.5 (2)	5.3 (4)	47 (3)	1000(5), 1413(7)
1625.5 (4)	0.7 (2)	7 (2)	-
1641.9 (3)	2.4 (3)	23 (3)	837(5)
1996.6 (4)	3.9 (3)	44 (4)	-
2443.3 (4)	2.4 (2)	31 (3)	-
2557.5 (3)	2.3 (2)	31 (4)	-
2896.0 (4)	0.9 (2)	14 (3)	-

and 2896 keV, which do not show any γ coincidences, are placed as ground-state transitions in this level structure based on spin and parity assignment considerations. These are discussed further below in this section.

By systematically shifting the relative excitation energy of both ^{65}Fe β-decay paths, it was checked that the non-coincident lines at 1441, 1626, 2443, 2558 and 2896 keV do not fit energy differences between states of the two structures simultaneously. As a result, two independent ^{65}Fe β-decay paths without mutual coincident transitions have been deduced from data set I pointing to the presence of two β-decaying states in ^{65}Fe. This is consistent with the recent discovery in Penning-trap mass measurements [50] of a long-lived isomer ($T_{1/2} > 150$ ms) at a 402-keV excitation energy in ^{65}Fe, presumably of high spin ($9/2^+$), while the ground state has low spin ($1/2^-$) [51]. Our gas cell is fast enough to allow detection of nuclei in the 100-ms range. Two other excited levels are known at a lower energy in ^{65}Fe; i.e., at 364 and 397 keV, respectively [52]. In the event that the 402-keV isomer does (partially) decay internally, a γ ray has to be observed at 363 or 402 keV in the singles γ spectrum, ignoring low-energy transitions. These transitions have not been observed in our ^{65}Fe decay study. A proof of the presence of two β-decaying states in ^{65}Fe would be the observation of γ rays with different half-lives. The decay behavior of γ rays belonging to the two different level schemes of Fig. 4 has been fitted by a single exponential function, shown in Figs. 5 and 6, resulting in half-life values of 1.12(15) s and 0.81(5) s, respectively. Previously determined half-life values of 0.45(15) s [53] and 1.3(3) s [17] were significantly different and Refs. [17, 50] already suggested the presence of a β-decaying isomer in ^{65}Fe to explain the discrepancy. However, the deduced half-life values are both longer than the value in Ref. [53] and, therefore, cannot be explained on this basis.

The relative energy position of the two level structures could not be derived from the experimental data. For this reason, it is a priori unclear whether both branches decay into a common ground state of ^{65}Co or if one of the branches decays into an isomeric state. In the latter case, the isomer has to reside at a relatively low excitation energy of $\sim$ 50 keV or less, since the Penning-trap mass measurements of Ref. [50] did not resolve an isomeric state in ^{65}Co. The relative ^{65}Ni γ intensities in data set I (lasers on iron) are found to be similar to those of data set II (lasers on cobalt). This is illustrated by the ratio of relative transition intensities $\frac{I_{rel}(II)}{I_{rel}(I)}$ from both data sets, see Table III. Because more than 90% of the

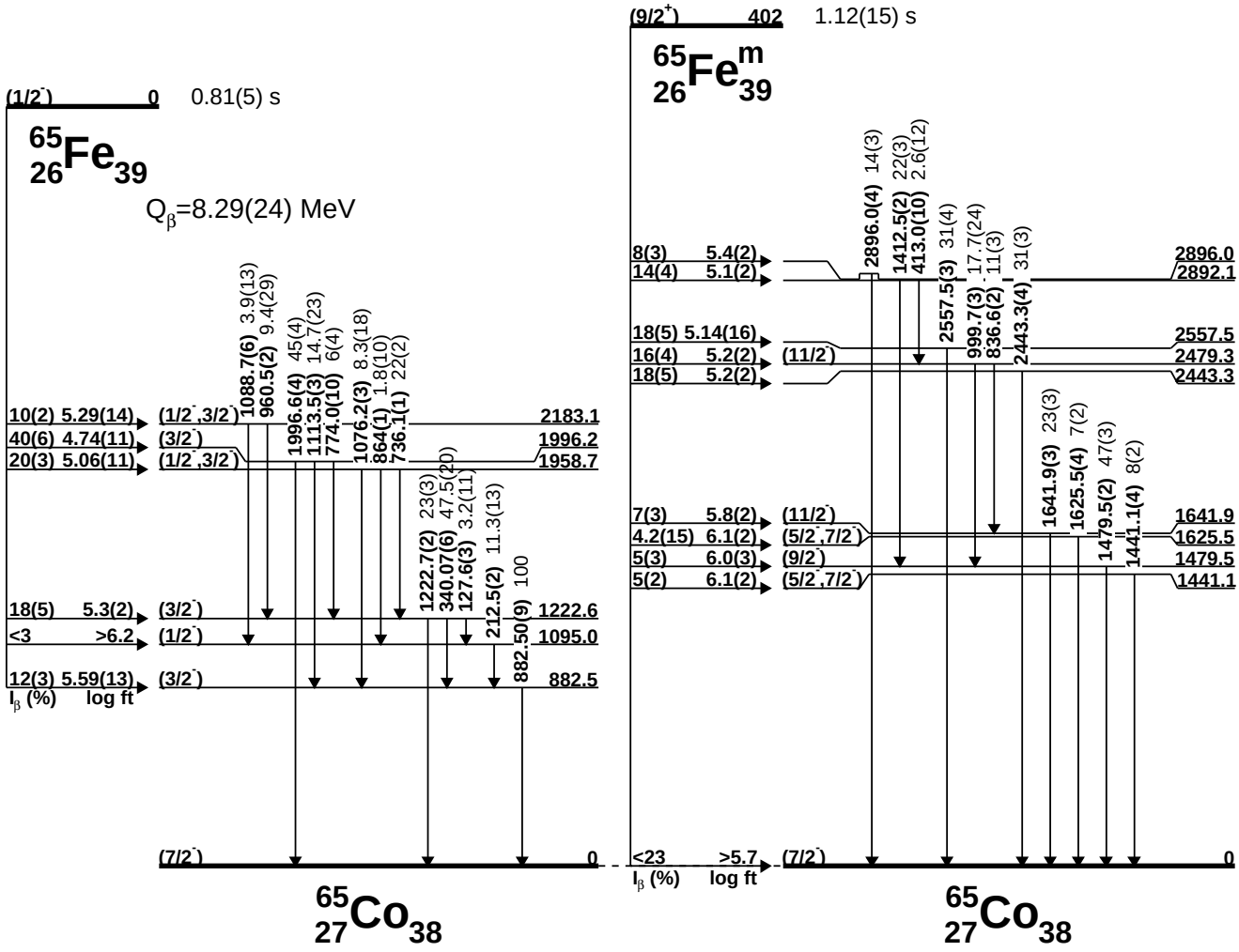

FIG. 4: The two ^{65}Fe decay schemes, see text for a detailed discussion.

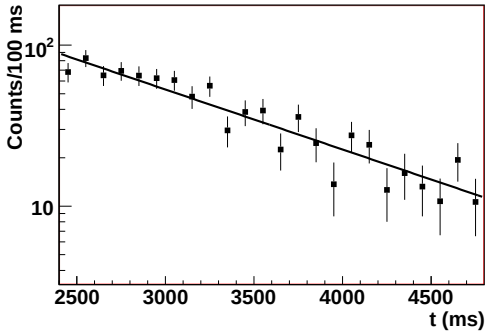

FIG. 5: Summed decay behavior with corresponding fit of the γ lines at 340, 736, 883 and 1997 keV, representative of the β decay of the ^{65}Fe ground state. The line represents a single exponential fit resulting in a half-life value of 0.81(5) s.

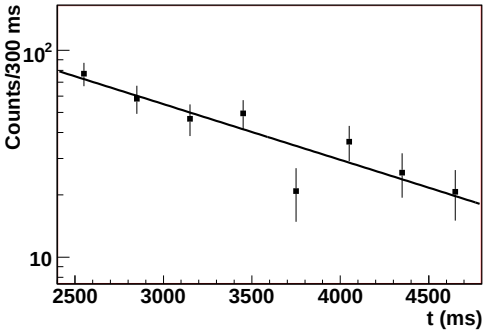

FIG. 6: Summed decay behavior with corresponding fit of the γ lines at 1000, 1413, 1480 and 1642 keV, representative of the β decay of the ^{65m}Fe isomer. The line represents a single exponential fit resulting in a half-life value of 1.12(15) s.

β feeding goes directly to the $5/2^-$ ground state, it has also been checked that the absolute γ intensity of the 310-keV transition belonging to the ^{65}Co decay is the same (within the uncertainties) in the direct ^{65}Co decay (data

set II) and via the ^{65}Fe decay (data set I). The fact that these ratios and the absolute γ intensity of the 310-keV transition are similar further supports the assumption of the presence of only one β-decaying state in ^{65}Co.

An intermediate conclusion here is that there is evidence for two excitation structures in ^{65}Co without any interconnecting transitions, fed by two β-decaying states in ^{65}Fe considerably differing in spin. Whether these level schemes are built on the same state and which one belongs to the decay of the high-spin (respectively low-spin) state needs further consideration. For the clarity of further discussion, we will attribute the left structure of Fig. 4 to the decay of the low-spin and the right structure to the high-spin state. This will be discussed in paragraph III B 3.

2. Deep-inelastic reaction at ANL

The β-decay data alone are insufficient to claim the (non-)existence of a β-decaying isomer in ^{65}Co with absolute certainty. Crucial information on the ^{65}Co level structure was extracted, however, from a deep-inelastic reaction study. In the present work, only the analysis of triple coincidence data (cubes) revealed useful results. As this type of reactions leads to the production of a wide range of projectile- and target-like fragments, the resulting complexity of the γ spectra can be resolved by using coincidence techniques. However, in the case of weakly-produced nuclei such as ^{65}Co, the analysis of γ-γ coincidence events did not provide spectra sufficiently clean to allow for the identification of new transitions and higher-order coincidences proved essential. Therefore, the success of the present analysis relied entirely on the high selectivity that could be achieved by analyzing triple gates in the coincidence cubes.

Excited levels in ^{65}Co were established by gating on any two coincident γ rays observed in the β-decay work reported in the previous section. The Radware [54] software package was used in the analysis. The study of triple coincidence data revealed the partial level scheme presented in Fig. 7. Examples of triple-coincidence spectra are found in Fig. 8. As seen in the spectra of Figs. 8c and 8d, the delayed triple-coincidence spectra contain much less statistics when compared to the prompt coincidence data given in the upper part of the same figure (8a and 8b). This is due to the fact that the observed delayed transitions result from the β decay of ^{65}Fe, which is only weakly produced in ^{64}Ni+^{238}U deep-inelastic reactions. The investigation of the delayed cube is expected to confirm levels in ^{65}Co reported in the previous section. On the other hand, the direct population of excited states can be studied by analyzing the prompt cube. In this case, the reaction mechanism favors the population of fairly high-spin yrast and near-yrast states, which might differ from those populated in β decay.

Indeed, the analysis of the delayed cube confirmed most of the levels observed in the β-decay work of Fig. 4. As already mentioned above, due to their high selectivity, only triple coincidences were used in the present study. Therefore, only cascades of three or more coincident γ rays observed in the β-decay work could be confirmed by the investigation of the deep-inelastic data set. As a consequence, the γ rays of 1076, 1114, 1223, and 1997 keV proposed to arise from the decay of the levels populated by the $(1/2^-)$ ground state of ^{65}Fe, see Fig. 4, and those of 1412, 1441, 1625, 2443, 2557 and 2896 keV believed to deexcite states populated in the decay of the $(9/2^+)$ isomer could not be investigated. The levels proposed in the β-decay work and confirmed by the analysis of the DDD cube are drawn with thin lines or marked with a star in the level scheme of Fig. 7.

The prompt population of the levels in the left part of Fig. 7 was studied by analyzing the PPP cube. No combination of gates set on transitions depopulating levels proposed (in the previous section) to receive feeding from the low-spin isomer in ^{65}Fe provided useful information. This indicates a very weak cross-section for direct population in a deep-inelastic reaction and suggests low-spin values for these levels.

The prompt double-gates, set on the 1000-1479 keV and 837-1642 keV cascades corresponding to the two different decay paths of the 2479-keV state, provided clear evidence for the presence of four low-energy coincident γ rays with energies of 190, 243, 359, and 447 keV, see Fig. 8a. Based on the results of the analysis of all possible combinations of double gates on the observed transitions, the new γ rays were arranged in the level scheme of ^{65}Co and deexcite from the levels represented with thick lines in Fig. 7. The 413-keV transition, observed in the β-decay work, and also confirmed in the analysis of the delayed cube to be in coincidence with the 1000-1479 keV and 837-1642 keV intense transitions (see Fig. 8c), was not observed in the PPP cube. This indicates that the 2892-keV state does not belong to the yrast or near-yrast sequence in ^{65}Co. The 2669-keV level identified in the prompt data was found to deexcite predominately via the 1190-keV transition (72% branching) to the 1479-keV level.

For this type of deep-inelastic reaction, angular correlation measurements are commonly used to determine the multipolarity of γ rays. However, in ^{65}Co, two of the strongest prompt transitions that could possibly be used as gates, e.g., the 1480- and 1190-keV γ rays, form a doublet with two intense lines in ^{69}Ga [55], a nucleus strongly produced in the present reaction. This prevents reliable multipolarity assignments for the new states identified in ^{65}Co in the deep-inelastic data set. Also, the statistics for the other observed transitions is too low to allow for an accurate angular-correlation analysis.

3. Spin and parity considerations and assignments

Unfortunately, the deep-inelastic data did not allow spin and parity assignments to be made on the basis of

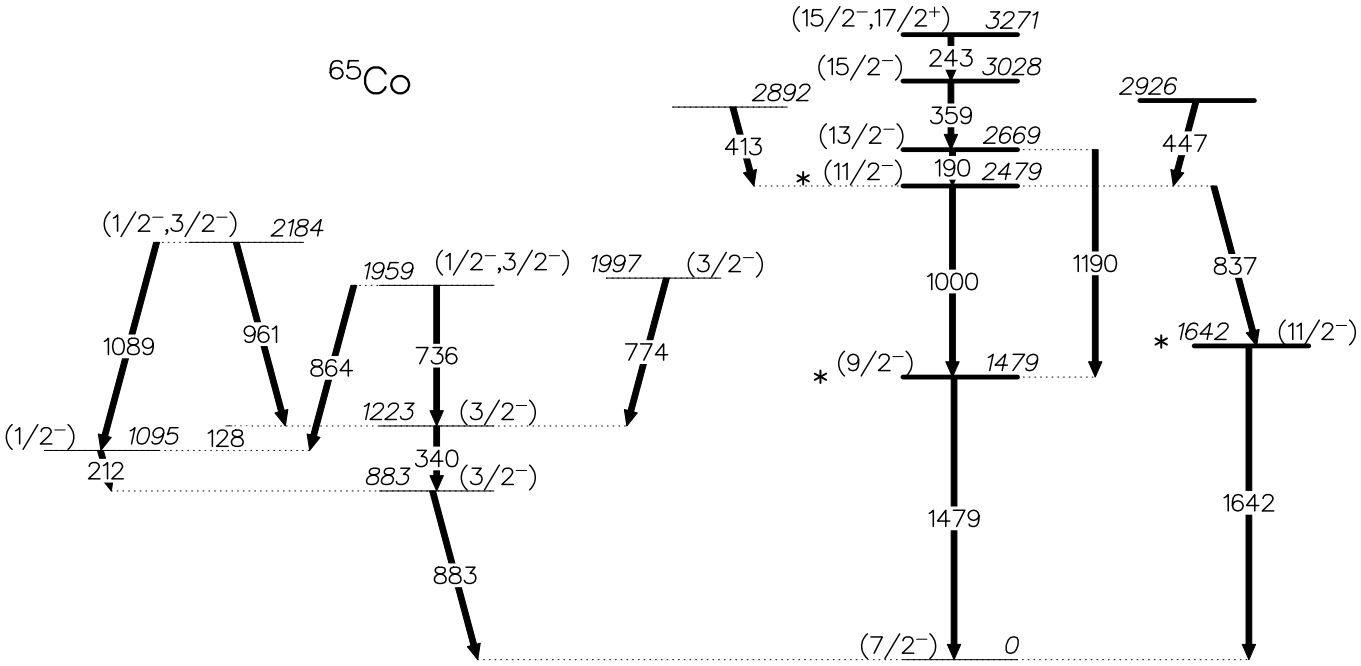

FIG. 7: ^{65}Co level scheme deduced from the ^{64}Ni+^{238}U deep-inelastic reaction by gating on any two coincident γ rays observed in the β decay of ^{65}Fe. Levels drawn with thick lines were observed in the analysis of the PPP cube, those represented with thin li ıd DDD c

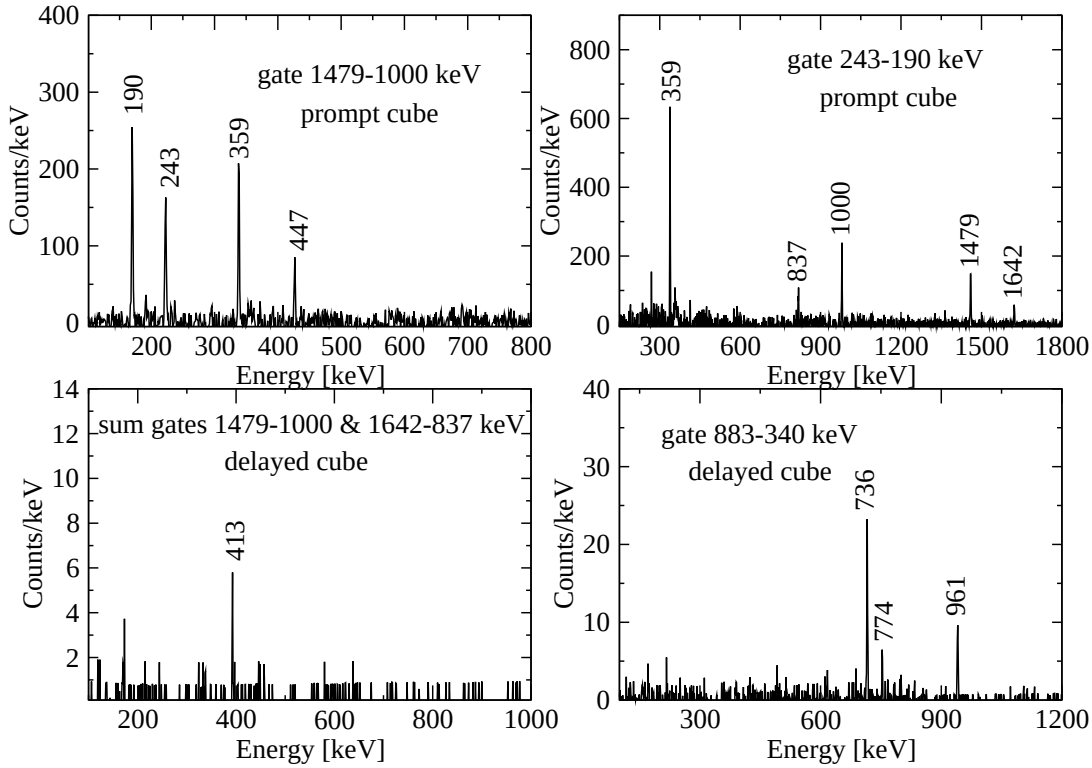

FIG. 8: Example of spectra from coincidence gates on transitions in ^{65}Co in prompt (a and b) and delayed cubes (c and d) with the data taken in the ^{64}Ni+^{238}U deep-inelastic reaction. Transitions in ^{65}Co are identified by their energies.

angular correlations. Thus, for the levels observed in the analysis of the delayed data and marked with a star in Fig. 7, spin and parities assigned in the β-decay work are assumed, as will be discussed further in this paragraph. However, a comparison with the near-yrast levels of ^{59}Co [56] and ^{61,63}Co [16] populated in other deep-inelastic reactions, reveals a strikingly similar low-energy structure, as can be noticed in Fig. 9. This suggests a $(7/2^-)$ ground state, and $(9/2^-)$, $(11/2^-)$ and $(11/2^-)$ levels at 1480, 1642 and 2479 keV, respectively. Note, however, that the 2479-keV level is also observed in the ^{65}Fe^m β-decay of the $(9/2^+)$ isomer with a low log ft value of 5.2(2). This value is inconsistent with the proposed negative parity. One should, nevertheless, also realize that the reported log ft values are essentially lower limits due to the possibility of unobserved γ-ray activity from high-energy levels. Because of the systematic similarity with the $^{59-63}$Co level structures obtained in deep-inelastic reactions, the $(11/2^-)$ assignment to the 2479-keV level is suggested. The states on top of this 2479-keV state most likely form the $(13/2^-)$, $(15/2^-)$ sequence, similarly to ^{61,63}Co [16] as can be seen in Fig. 9, but positive parity cannot be entirely disregarded. It is worth mentioning that 15/2 is the maximum spin value of negative parity that can be achieved within the $\pi f_{7/2}^{-1}\nu(p_{3/2}f_{5/2}p_{1/2})^{-2}$ configuration. The highest observed level at 3271 keV might have either J^π=17/2$^+$ or 15/2$^-$.

In the deep-inelastic data there is also no linking transition observed between the low-spin levels (left part of Fig. 7) and the high-spin levels (right part of Fig. 7). They are placed, as in Fig. 4, on the $(7/2^-)$ ground state of ^{65}Co, as the only argument for a low-spin isomer in ^{65}Co, the feeding of the previously $(1/2^-)$ assigned 1274-keV level in ^{65}Ni [48], has been argued against in paragraph III A.

In Fig. 4, all the states fed by the $(1/2^-)$ ^{65}Fe ground state (log $ft \leq 5.6(2)$), and subsequently decaying towards the $(7/2^-)$ ground state, can be assigned as $(3/2^-)$ levels; i.e., the states at 883, 1223 and 1996 keV. Allowed Gamow-Teller transitions and γ transitions with multipolarity less than three are assumed. The states at 1959 and 2183 keV are also significantly fed in β decay from the $(1/2^-)$ ground state, but their decay towards the $(7/2^-)$ ^{65}Co ground state is not observed. It is tempting to assign these states a spin and parity of $1/2^-$, but from Weisskopf estimates, a $3/2^-$ assignment cannot be ruled out. The state at 1095 keV is fed by low-spin levels and decays preferentially into the $(3/2^-)$ state at 883 keV rather than towards the $(7/2^-)$ ground state. Hence, a $(1/2^-)$ assignment is tempting, but again $(3/2^-)$ cannot be disregarded. Note also that the 1095-keV level is not fed in β decay, pointing to the fact that its structure is significantly different from the other observed low-spin states; see also section IV B for more details.

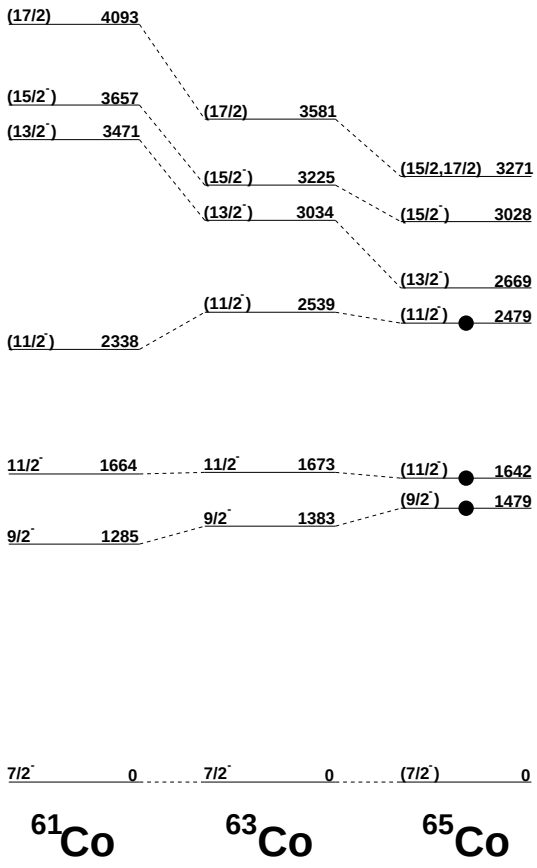

FIG. 9: Yrast and near-yrast levels in odd-mass $^{61-65}$Co that are systematically populated in deep-inelastic reactions. The ^{65}Co levels at 1479, 1642, and 2479 keV, respectively, are also observed in the β decay of the ^{65}Fe isomer (full circle). The levels of ^{61,63}Co are taken from Ref. [16].

C. ^{67}Fe decay to ^{67}Co

Fig. 10(a) presents the vetoed, β-gated γ spectra from data set IV with the lasers tuned resonantly to iron in black and from data set V with the lasers off normalized to the laser-on time in red. Fig. 10(b) provides the vetoed, β-gated γ spectra from data set VI with the lasers tuned resonantly to iron in black and from data set VII with the lasers off normalized to the laser-on time in red. The full circles indicate lines from ^{67}Fe, open squares from ^{67}Co and open triangles from contaminant β decay. From data set IV the ^{67}Fe half-life was extracted with a single exponential fit of the 189-keV time dependence during the decay period ($T_{1/2}$ = 416(29) ms) [23]. From data set VI the ^{67}Co level scheme was constructed [23].

Lines present in the spectra with the lasers on and absent with the lasers off can unambiguously be identified as coming from ^{67}Fe β decay. The isomeric behavior of a laser-enhanced line at 492 keV was already evidenced and

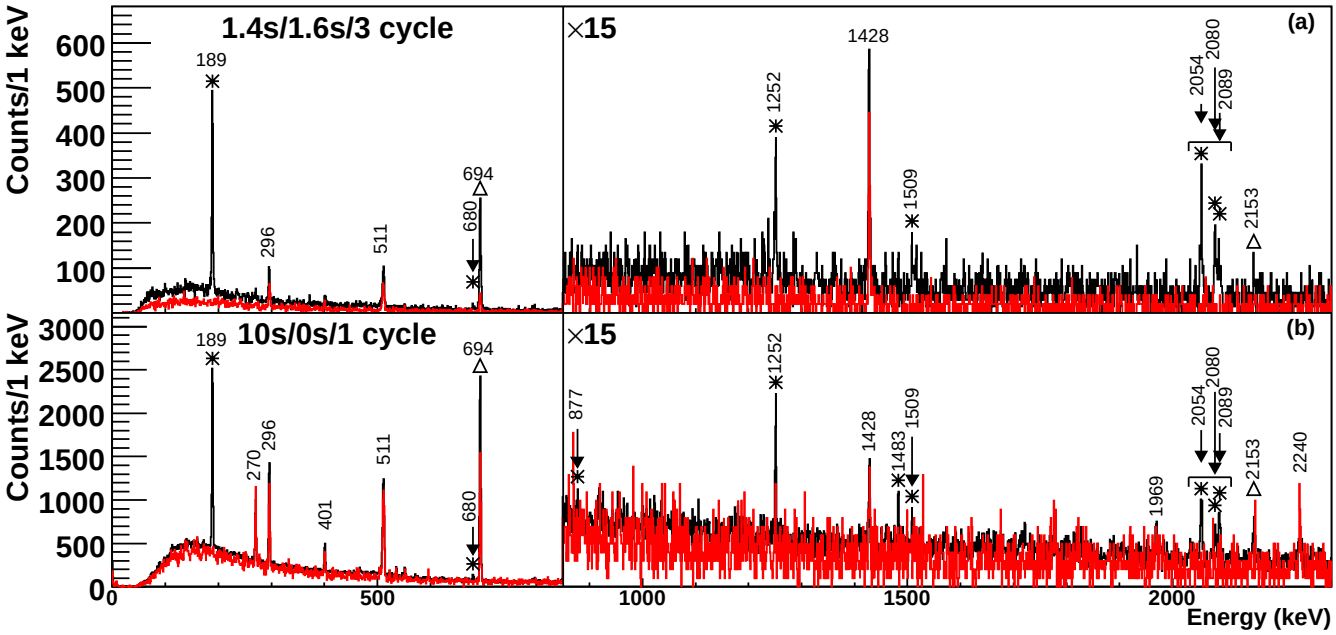

FIG. 10: The vetoed, β-γ spectrum with the lasers tuned to ionize iron in black and with the lasers off normalized to the laser-on time in red (on-line version only) in the 1.4s/1.6s/3 cycle (top, data sets IV and V, respectively) and the 10s/0s/1 cycle (bottom, data sets VI and VII, respectively). The lines from ^{67}Fe β decay are marked with a star and those from ^{67}Co with an open triangle. Contaminant lines are not marked, see in the text for further information.

extensively discussed in Ref. [23]. The most intense transitions in the ^{67}Fe decay have energies of 189, 492, 680, 1252, 1483, 1509, 2054, 2080 and 2089 keV. The strong γ line at 694 keV originates from ^{67}Co β decay [7]. The contaminant lines are originating from doubly-charged molecules. The lines at 270, 1969 and 2240 keV are from the decay of ^{106}Tc; the lines at 296 and 401 keV from ^{102}Nb; and the line at 1428 keV from ^{94}Sr. Molecules are formed with CO, O_2 and ^{40}Ar, respectively.

The 492-keV and 680-keV levels have already been established from correlations measured in the seconds time range [23]. However, the construction of the higher-energy structure of ^{67}Co, given in Fig. 12, has not been discussed in detail yet. A solid basis is given by the γ spectrum of coincident 189-keV events, shown in Fig. 11. The coincident 571-keV line and a 1252-keV cross-over γ ray give evidence for the state at 1252 keV. The 1859-keV state is placed, based on the 1179-keV line in the spectrum of Fig. 12 together with the, albeit weak, 1368-keV cross-over transition. Evidence for a 2735-keV level is delivered by the 189-keV γ ray being coincident with the 2054-keV line and the presence of the 877-keV and 1483-keV events, which are coincident with 1179-keV and 1252-keV events, respectively. The 2761-keV state could be established from the 189-keV γ ray being coincident with the 2080-keV line and the 1509-keV events being coincident with 1252-keV events. The level at 2769 keV, finally, is placed on the basis of the 2089-keV line in the spectrum of Fig. 11. The spectrum also indicates an intense peak at 505 keV (marked with "$694-189$"), which contains the 189-keV coincident Compton events originating from the 694-keV transition.

The γ intensities indicated in Fig. 12 are relative to the 189-keV transition ($I_\gamma = 100$). The assigned transitions, count rates and relative intensities are summarized in Table V. The data do not leave room for β feeding towards the ^{67}Co ground state by comparing the total γ intensity of ^{67}Co and ^{67}Ni. The β feeding towards the excited ^{67}Co states is based on missing γ intensities. As can be seen in Fig. 12, the total feeding is shared $50-50$ between the state at 680 keV and the group of levels at 2769, 2761 and 2735 keV. It is remarkable that the latter group of states decays to the level at 680 keV, but not towards the ground state nor the state at 492 keV. Therefore, Table V also provides upper limits (95% confidence limit) for the respective cross-over transitions. Compared to the 2054-keV transition, all the cross-over transitions, except for the 2243-keV γ ray, are at least 4 times weaker. The larger upper limit for the 2243-keV transition is due to the presence of a ^{106}Tc contamination at 2240 keV. The transitions at 571, 877, 1179 and 1368 keV were firmly assigned to the ^{67}Fe β decay following the inspection of the observed β-γ-γ coincidences. The isomeric 492-keV state has been fully characterized by correlations with β-gated 189- and 694-keV γ events.

The spins and parities of the four lowest ^{67}Co levels are assigned in Ref. [23]. The ^{67}Fe ground state was initially assigned a spin and parity of $J^\pi = (5/2^+)$ from isomeric ^{67m}Fe γ decay [57], but this would be inconsistent with the strong β branch towards the $(3/2^-)$ state at 680 keV.

TABLE V: ^{67}Co transitions from data set IV are indicated by their energy E (keV), the corresponding off resonant subtracted peak count rate A_γ corrected for β efficiency and γ intensity I_{rel} relative to the 189-keV transition (100 %). The last six lines give upper γ-intensity limits (95 % confidence limit) of important transitions. Multiply I_{rel} by 0.847 (36) to get absolute γ intensities. The γ energies of coincident events are listed in the last column with the number of observed β-γ-γ coincidences between brackets.

E (keV)	A_γ (cts/h)	I_{rel} (%)	Coincident $\beta\gamma$-events
188.93 (8)	186 (6)	100	571(22), 877(7), 1179(10), 1483(5), 2054(34), 2080(10), 2089(29)
491.55 (11)	99 (15)	99 (29)	-
571.4 (2)	3.4 (10)	3.7 (14)	189(17), 1483(1), 1509(3)
680.4 (2)	6.6 (11)	8 (3)	-
876.9 (6)	3.4 (10)	5 (2)	189(9), 1179(5), 1368(2)
1178.9 (3)	1.9 (6)	3.3 (14)	189(7), 877(5)
1251.9 (4)	5.4 (19)	10 (4)	1483(6), 1509(4)
1368.0 (10)	0.5 (4)	1.1 (9)[a]	877(2)
1483.2 (2)	3.4 (7)	7 (2)	189(5), 571(1), 1252(6)
1508.9 (3)	3.8 (8)	8 (3)	189(1), 571(3), 1252(4)
2054.2 (2)	6.9 (9)	18 (5)	189(35)
2079.8 (5)	3.3 (9)	8 (3)	189(14)
2088.7 (2)	6.3 (9)	16 (5)	189(29)
2243.3 (2)	-	< 10	-
2269.0 (3)	-	< 3.9	-
2277.6 (2)	-	< 3.3	-
2734.8 (2)	-	< 4.5	-
2760.6 (3)	-	< 4.4	-
2769.2 (2)	-	< 0.9	-

[a]The relative intensity is based on the number of coincidences with β-gated 877-keV γ rays.

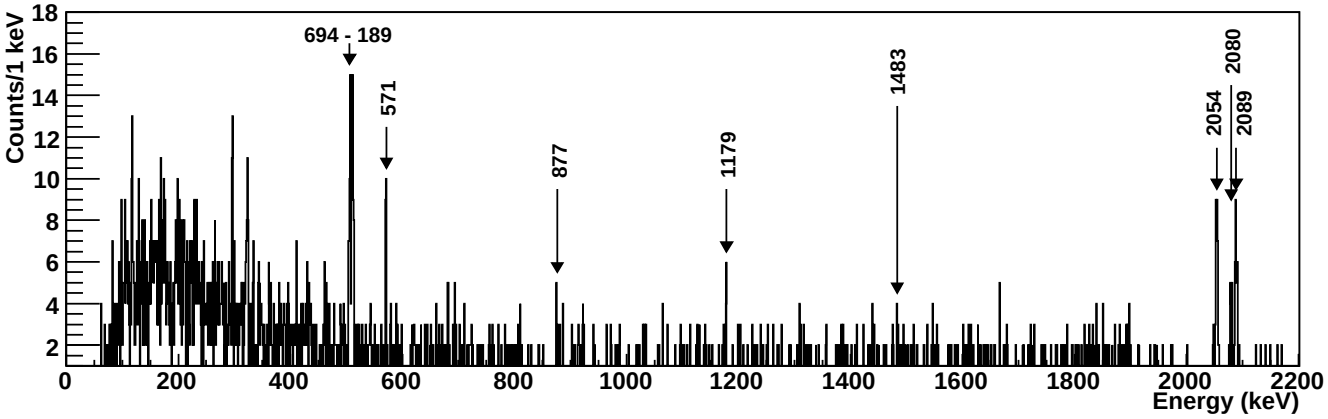

FIG. 11: The γ spectrum of prompt coincidences with β-gated 189-keV events (from data set VI). The structure indicated by $694 - 189$ is due to Compton scattering of the 694-keV line.

On the other hand, a $(1/2^-)$ assignment for the ^{67}Fe ground state, as proposed in Ref. [50], is in agreement with the proposed level scheme. It also explains the lack of feeding towards both the $(7/2^-)$ ground state and the 1252-keV $(5/2^-)$ level. The low log ft limit of 5.4 for the β feeding of the $(1/2^-)$ isomer will be discussed in next section. The strong β decay towards the states at 2735 (log $ft = 4.8(2)$), 2761 (log $ft = 5.0(2)$) and 2769 keV (log $ft = 5.0(2)$) gives strong support for spin and parity of $(1/2^-)$ or $(3/2^-)$.

The 2735- and 2761-keV levels are observed to decay to the $(5/2^-)$ state at 1252 keV with an intensity similar to that feeding the $(3/2^-)$, 680-keV level, while the 2769-keV level is only observed to decay to the 680-keV state and not to the 1252-keV level. From Weisskopf estimates, E2 and M1 transitions from the 2.75-MeV levels towards the 1252-keV state are, respectively, three orders of magnitude and two times less probable than M1 transitions to

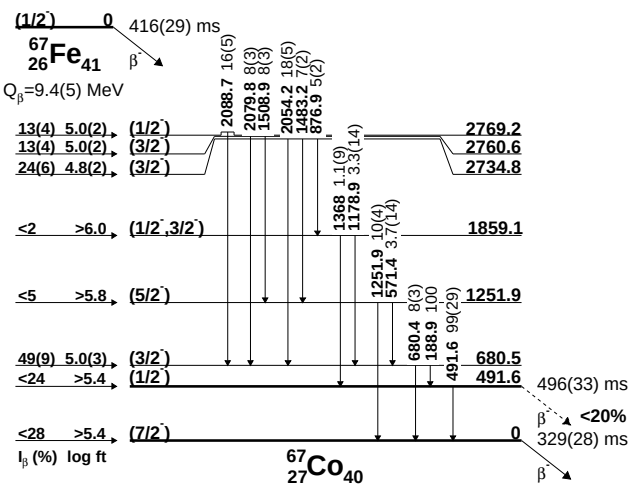

FIG. 12: Partial ^{67}Co level scheme. Multiply the relative γ intensities by 0.85(4) to obtain absolute γ strengths.

the 680-keV level. Hence, the 2735- and 2761-keV states can tentatively be assigned a $(3/2^-)$ spin and parity and the 2769-keV level $(1/2^-)$ quantum numbers. The state at 1859 keV is observed to decay to both the $(3/2^-)$ state at 680 keV and the $(1/2^-)$ level at 492 keV and not to the $7/2^-$ ground state. This restricts its spin and parity to $1/2^-$ or $3/2^-$, despite the lack of direct β feeding from the ^{67}Fe ground state.

IV. INTERPRETATION

A. Levels in ^{65}Ni

The ^{65}Co ground state has spin and parity $(7/2^-)$, which arises from the $\pi f_{7/2}^{-1}$ proton-hole. The dominant β-decay path is the Gamow-Teller conversion of a $f_{5/2}$-neutron into a $f_{7/2}$-proton feeding states in ^{65}Ni, which can be interpreted as a $\nu f_{5/2}^{-1}$ neutron-hole coupled to ^{66}Ni. By far, the strongest β strength is observed toward the $5/2^-$ ground state, which can be interpreted rather naturally as the $\nu f_{5/2}^{-1}$ neutron-hole state.

The other levels that are fed in β decay reside at an excitation energy of 1141 and 1274 keV, which are tentatively assigned $(7/2^-, 9/2^-)$ and $(5/2^-)$ spin and parity, respectively. The low-energy level structure of ^{65}Ni can then be interpreted as a $\nu f_{5/2}^{-1}$, $\nu p_{1/2}^{-1}$ or $\nu p_{3/2}^{-1}$ neutron-hole coupled to the ^{66}Ni level structure. The $1/2^-$ state at 63 keV is the $\nu p_{1/2}^{-1}$ neutron-hole state and the $3/2^-$ level at 310 keV is the $\nu p_{3/2}^{-1}$ neutron-hole state. The 1274-keV and the 1141-keV levels can be interpreted as the coupling of the $\nu f_{5/2}^{-1}$ hole to the 2^+ state in ^{66}Ni, which lies at 1426 keV (see Fig. 13).

B. Levels in ^{65}Co

As will be discussed in this paragraph, ^{65}Co can be interpreted in terms of two coexisting structures. On the one hand, states are suggested arising from a $\pi f_{7/2}^{-1}$ proton hole coupled to the first excited 2_1^+ and 3_1^+ states of the ^{66}Ni core, see Fig. 13. On the other hand, the $(1/2^-)$ state at 1095 keV is suggested to arise from proton excitations across the $Z = 28$ shell closure. This assignment is based on the similarity with the established $(1/2^-)$ proton intruder state in ^{67}Co, which is observed in the ^{67}Fe β decay [23]. In addition, the comparison with the ^{67}Co structure indicates that the $(3/2^-)$ state at 1223 keV can be interpreted as the first member of the rotational band built on top of the $(1/2^-)$ proton intruder state.

The most straightforward configuration of the suggested $(1/2^-)$ ^{65}Fe ground state [50] is $\pi f_{7/2}^{-2} \nu p_{1/2}^{-1}$. This assignment is, indeed, consistent with the ground state of the ^{66}Co isotone, which is proposed to be the 3^+ member of the $\pi f_{7/2}^{-1} \nu p_{1/2}^{-1}$ configuration [8, 58]. For both isotones, the preferred decay mode is a Gamow-Teller conversion of a $f_{5/2}$-neutron into a $f_{7/2}$-proton [8]. Since the dominant neutron configuration is identical in the two isotones, a similar β-decay pattern is expected for both cases. In the ^{66}Co β decay, two levels at 2672 and 3228 keV with a dominant $\nu p_{1/2}^{-1} \nu f_{5/2}^{-1}$ configuration, coupling to a respective spin and parity of 2^+ or 3^+, are strongly fed [8]. In the ^{65}Fe β decay, strong allowed Gamow-Teller decay is expected to $J^\pi = 1/2^-$ and/or $3/2^-$ states with a dominant $\pi f_{7/2}^{-1} \nu p_{1/2}^{-1} \nu f_{5/2}^{-1}$ configuration, which is a $\pi f_{7/2}^{-1}$ proton-hole coupled to the strongly fed 2^+ or 3^+ states of ^{66}Ni.

The strongest feeding is observed to the $(3/2^-)$ level at 1996 keV with a log ft value of 4.74(11). This is very similar to the log ft value of 4.2(5) of the ^{66}Co β decay towards the 3^+ state at 2670 keV [8]. On this basis, the 1996-keV state in ^{65}Co can be interpreted as arising from a coupling of the $\pi f_{7/2}^{-1}$ proton hole with the 3^+ state, and a large percentage of the $\pi f_{7/2}^{-1} \nu p_{1/2}^{-1} \nu f_{5/2}^{-1}$ configuration is assigned, as depicted in Fig. 13. One of the states at either 1959 or 2183 keV may well be the $1/2^-$ member of the multiplet, but, in this case, the higher log ft values indicate that the proposed configuration is less dominant than in the $3/2^-$ member.

The high-spin members of the $\pi f_{7/2}^{-1} \nu p_{1/2}^{-1} \nu f_{5/2}^{-1}$ multiplet are not fed in the β decay of the $(1/2^-)$ ground state and should rather be searched for in the decay of the $9/2^+$, ^{65}Fe^m isomer. The $(9/2^+)$ ^{65}Fe isomeric state, however, has to involve the $\nu g_{9/2}^{+1}$ configuration and, similar to the $(1/2^-)$ ground state, the Gamow-Teller conversion of a $f_{5/2}$-neutron into a $f_{7/2}$-proton is expected to be the preferred decay mode. The 2479-keV state is, despite its apparent low log ft value, tentatively assigned $(11/2^-)$ and the 2669-keV level tentatively $(13/2^-)$, which would be the highest possible spin

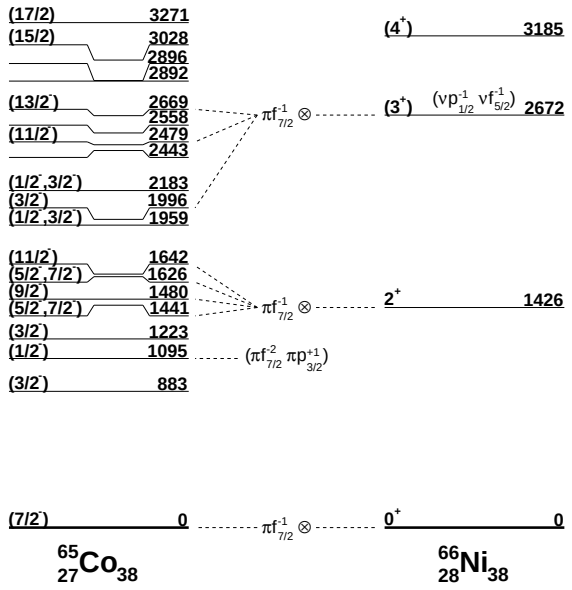

FIG. 13: The ^{65}Co levels interpreted as proton-hole states coupled to ^{66}Ni coexisting with a proton intruder state at 1095 keV.

formed by a $\pi f_{7/2}^{-1} \otimes 3^+$ coupling. There is, however, no further evidence to support such an interpretation.

The states at 1480 and 1642 keV were assigned $(9/2^-)$ and $(11/2^-)$, respectively, from the systematics of ^{59,61,63}Co structures revealed in deep-inelastic experiments [16, 56]. Since the configuration of the $(9/2^-)$ and $(11/2^-)$ states in the lighter cobalt isotopes were identified as corresponding to a coupling of $\pi f_{7/2}^{-1}$ with the first excited 2_1^+ state [59], it is tempting to assign the same configuration to the 1480- and 1642-keV states. The 2_1^+ excitation energy in ^{66}Ni of 1425 keV and the observed weak β decay from the $(9/2^+)$ isomer to these levels is consistent with this interpretation. Two other states, at 1441 and 1626 keV, exhibit similar excitation energies and β-decay strengths, see Fig. 4, which indicate that these might be other members of the multiplet. A first-forbidden decay from the $(9/2^+)$ level can only feed levels with $J \geq 5/2$. Moreover, the 1441- and 1626-keV states are only observed to decay to the $(7/2^-)$ ground state. Hence, they are good candidates for the $5/2^-$ and $7/2^-$ members of the multiplet. The only missing member of the multiplet, at this point, is the $3/2^-$ level, but with the $(3/2^-)$ levels at 883 and 1223 keV, there are two possible candidates in this case as well.

Both $(3/2^-)$ states are rather strongly fed by direct β decay, but the $(1/2^-, 3/2^-)$ level at 1095 keV gets almost no β feeding ($\log ft > 6.2$) and, therefore, must be associated with a fundamentally different configuration. This low-energy structure is very similar to the one seen in ^{67}Co, where the β decay is strongly hindered to a $(1/2^-)$ state at 492 keV, which was interpreted as a $\pi(1p-2h)$ intruder state [23]. Analogously, the 1095-keV level is most likely a deformed $(1/2^-)$ state involving proton excitations across $Z = 28$. As in ^{67}Co, the intruder state appears low in energy because of strong attractive proton-neutron residual interactions [60], that are maximized by the weakening of the $N = 40$ subshell closure.

From this point of view, the first excited $(3/2^-)$ level can be interpreted as the $\pi f_{7/2}^{-1}$ coupling to the 2_1^+ state, and the second excited $(3/2^-)$ level as the first rotational band member of the $(1/2^-)$ proton intruder, in analogy with ^{67}Co. Nevertheless, both states are significantly fed in ^{65}Fe β decay with respective $\log ft$ values of 5.59(13) and 5.3(2). Their similar strengths indicate significant configuration mixing for both levels. With the 883-, 1441-, 1480-, 1626-, and 1642-keV states interpreted as members of the $\pi f_{7/2}^{-1} \otimes 2^+$ quintet, coexisting with the 1095- and 1223-keV states interpreted as proton intruder configurations, we describe all levels below 1.7 MeV.

C. Levels in ^{67}Co

The ^{67}Fe ground state requires, contrary to ^{65}Fe, excitations across $N = 40$ to account for its $(1/2^-)$ spin and parity. In fact, the ground state of the ^{68}Co isotone has been interpreted as associated with a $\pi f_{7/2}^{-1} \nu g_{9/2}^{+2} \nu p_{1/2}^{-1}$ configuration [8]. Hence, the ground state of ^{67}Fe consists most likely of a dominant $\pi f_{7/2}^{-2} \nu g_{9/2}^{+2} \nu p_{1/2}^{-1}$ configuration and, as in the $A = 65$ case discussed in the previous paragraph, one should expect a similar ^{68}Co and ^{67}Fe β-decay pattern of a $\nu f_{5/2} \rightarrow \pi f_{7/2}$ allowed Gamow-Teller conversion. However, the ^{68}Co β-decay study revealed that there is no level in ^{68}Ni with a dominant $\nu g_{9/2}^{+2} \nu f_{5/2}^{-1} \nu p_{1/2}^{-1}$ configuration in its wave function. In ^{68}Ni, two levels at 4027 and 4165 keV were interpreted as arising from this multiplet, but with considerable mixing with the $\pi f_{7/2}^{-1} \pi p_{3/2}^{+1}$ configuration. Therefore, the β-decay pattern of ^{67}Fe and ^{68}Co may not be as strikingly similar as in the case of ^{65}Fe and ^{66}Co.

Strong feeding is observed to three levels at $\sim$ 2.75 MeV with low $\log ft$ values of ~ 5.0. This compares well with the β decay of the ^{65}Fe ground state to three levels at $\sim$ 2 MeV, and is indicative of their structure consisting of a dominant $\pi f_{7/2}^{-1} \nu g_{9/2}^{+2} \nu f_{5/2}^{-1} \nu p_{1/2}^{-1}$ configuration. However, the γ decay in ^{65}Co and ^{67}Co is substantially different. In Figs. 4 and 10 it can be noticed, for instance, that the 1996-keV level in ^{65}Co strongly decays towards the ground state, while no ground state transitions have been observed from any of the $\sim$ 2.75-MeV levels in ^{67}Co. Thus, there appears to also be a significant structural change when going from the $N = 38$ nucleus, ^{65}Co, to the $N = 40$ nucleus, ^{67}Co. The low-energy states at 680 and 1252 keV have been discussed already in previous work [23] and were interpreted as the first members of a rotational band built on the $(1/2^-)$ proton intruder state.

V. CONCLUSIONS

The mass $A = 65$ β-decay chain from iron down to nickel and the ^{67}Fe β decay have been investigated at the LISOL facility. The ^{65}Co structure has been studied in detail from the combined analysis of β decay and complementary deep-inelastic data, which were taken at ANL. A new ^{65}Fe and a more detailed ^{67}Fe decay scheme have been presented and discussed.

The β decay of ^{65}Fe is feeding two independent level structures originating from a $(1/2^-)$ ground state and a $(9/2^+)$ isomeric state. The half-lives of both states have been determined as $T_{1/2} = 0.81(5)$ s and $T_{1/2} = 1.02(14)$ s, respectively. The deduced ^{65}Co structure can be interpreted as arising from the coupling of a $\pi f_{7/2}^{-1}$ proton-hole state with core levels of ^{66}Ni, coexisting with a proton intruder state at 1095 keV.

The subsequent β decay of ^{65}Co is revisited in the present work. Apart from the wrongly assigned 883- and 340-keV transitions, which are now unambiguously placed in the ^{65}Fe decay scheme, the ^{65}Co decay scheme is found to be consistent with that proposed in Ref. [22]. The two independent level structures observed in the ^{65}Fe β decay are placed on one common $(7/2^-)$ ground state. As a consequence, we claim that the previous $1/2^-$ assignment of the 1274-keV level in ^{65}Ni [48] is incorrect. Instead, a $(5/2^-)$ spin and parity is suggested. The observed low-energy structure of ^{65}Ni is interpreted as arising from $\nu f_{5/2}^{-1}$, $\nu p_{1/2}^{-1}$ and $\nu p_{3/2}^{-1}$ neutron-hole configurations coupled to the ^{66}Ni core structure.

The ^{65}Fe and ^{67}Fe ground states feature similar β-decay patterns. Strong feeding is observed to three high-energy $(1/2^-), (3/2^-)$ nickel core-coupled states arising from $\nu p_{1/2}^{-1} f_{5/2}^{-1}$ and $\nu g_{9/2}^{+2} p_{1/2}^{-1} f_{5/2}^{-1}$ neutron configurations, respectively, and to a $(3/2^-)$ level suggested to arise from a proton intruder configuration, which in the case of ^{65}Co is strongly mixed with the 2^+ core-coupled configuration. However, there is also evidence for structural changes between ^{65}Co and ^{67}Co. A strong transition was observed in ^{65}Co from the 1996-keV level to the spherical $(7/2^-)$ ground state, whereas the analogous ground state transition was not observed from any of the ~ 2.75-MeV levels in ^{67}Co. The structure could not be discussed quantitatively due to the lack of reliable large-scale shell model calculations. Nevertheless, it is clear that low-energy proton intruder configurations are now observed from $N = 38$ onwards due to the strong tensor interaction between the $\pi f_{7/2}^{-1}$ proton hole and the $\nu f_{5/2}$ and $\nu g_{9/2}$ orbitals, demonstrating how subtle the $N = 40$ subshell gap is.

Acknowledgments

We gratefully thank J. Gentens and P. Van den Bergh for running the LISOL separator and we acknowledge the support by the European Commission within the Sixth Framework Programme through I3-EURONS (contract no. RII3-CT-2004-506065), BriX-IUAP P6/23, FWO-Vlaanderen (Belgium), GOA/2004/03, the Foundation for Polish Science (A.K.), the U.S. Department of Energy, Office of Nuclear Physics, under Contracts DEFG02-94ER40834 and DE-AC02-06CH11357, and the Alexander von Humboldt Foundation (W.B.W.).

[1] M. Bernas et al., Phys. Lett. B **113**, 279 (1982).
[2] R. Broda et al., Phys. Rev. Lett. **74**, 868 (1995).
[3] T. Pawlat et al., Nucl. Phys. A **574**, 623 (1994).
[4] R. Grzywacz et al., Phys. Rev. Lett. **81**, 766 (1998).
[5] S. Franchoo et al., Phys. Rev. Lett. **81**, 3100 (1998).
[6] W. F. Mueller et al., Phys. Rev. Lett. **83**, 3613 (1999).
[7] L. Weissman et al., Phys. Rev. C **59**, 2004 (1999).
[8] W. F. Mueller et al., Phys. Rev. C **61**, 054308 (2000).
[9] J. Van Roosbroeck et al., Phys. Rev. C **69**, 034313 (2004).
[10] B. Zeidman and J.A. Nolen, Jr, Phys. Rev. C **18**, 2122 (1978).
[11] G. Georgiev et al., J. Phys. G **28**, 2993 (2002).
[12] O. Sorlin et al., Phys. Rev. Lett. **88**, 092501 (2002).
[13] N. Bree et al., Phys. Rev. C **78**, 047301 (2008).
[14] I. Stefanescu et al., Phys. Rev. Lett. **98**, 122701 (2007).
[15] I. Stefanescu et al., Phys. Rev. Lett. **100**, 112502 (2008).
[16] P. H. Regan, J. W. Arrison, U. J. Hüttmeier, and D. P. Balamuth, Phys. Rev. C **54**, 1084 (1996).
[17] O. Sorlin et al., Nucl. Phys. A **669**, 351 (2000).
[18] M. Sawicka et al., Eur. Phys. J. A **22**, 455 (2004).
[19] M. M. Rajabali et al., in *Proceedings of the Fourth International Conference on Fission and Properties of Neutron-Rich Nuclei*, edited by J. H. Hamilton, A. V. Ramayya, and H. K. Carter (Sanibel Island, USA, 2007), p. 679.
[20] L. Gaudefroy, Ph.D. thesis, Université de Paris XI Orsay (2005).
[21] N. Hoteling et al., Phys. Rev. C **74**, 064313 (2006).
[22] U. Bosch et al., Nucl. Phys. A **477**, 89 (1988).
[23] D. Pauwels et al., Phys. Rev. C **78**, 041307(R) (2008).
[24] T. Otsuka, T. Suzuki, R. Fujimoto, H. Grawe, and Y. Akaishi, Phys. Rev. Lett. **95**, 232502 (2005).
[25] E. Caurier, F. Nowacki, and A. Poves, Eur. Phys. J. A **15**, 145 (2002).
[26] O. Sorlin et al., Eur. Phys. J. A **16**, 55 (2003).
[27] N. A. Smirnova, A. De Maesschalck, A. Van Dyck, and K. Heyde, Phys. Rev. C **69**, 044306 (2004).
[28] M. Hjorth-Jensen, T.T.S. Kuo, and E. Osnes, Phys. Rep. **261**, 125 (1995).
[29] F. Nowacki, Ph.D. thesis, IReS, Strasbourg (1996).
[30] M. Hannawald et al., Phys. Rev. Lett. **82**, 1391 (1999).
[31] P. Adrich et al., Phys. Rev. C **77**, 054306 (2008).
[32] N. Aoi et al., Nucl. Phys. A **805**, 400c (2008).
[33] S. Rahaman et al., Eur. Phys. J. A **34**, 5 (2007).
[34] G. Audi, A. H. Wapstra, and C. Thibault, Nucl. Phys. A **729**, 337 (2003).
[35] T. Otsuka, T. Matsuo, and D. Abe, Phys. Rev. Lett. **97**, 162501 (2006).

[36] J. Hakala et al., Phys. Rev. Lett. **101**, 052502 (2008).
[37] A. M. Oros-Peusquens and P. F. Mantica, Nucl. Phys. A **669**, 81 (2000).
[38] Y. Kudryavtsev et al., Nucl. Instr. Meth. Phys. Res. B **204**, 336 (2003).
[39] M. Facina et al., Nucl. Instr. Meth. Phys. Res. B **226**, 401 (2004).
[40] P. Van den Bergh et al., Nucl. Instr. Meth. Phys. Res. B **126**, 194 (1997).
[41] J. Eberth et al., Prog. in Part. and Nucl. Phys. **46**, 389 (2001).
[42] D. Pauwels et al., Nucl. Instr. Meth. Phys. Res. B **266**, 4600 (2008).
[43] L. Weissman et al., Nucl. Instr. Meth. Phys. Res. A **423**, 328 (1999).
[44] N. Hoteling et al., Phys. Rev. C **77**, 044314 (2008).
[45] I. Y. Lee, Nucl. Phys. A **520**, c641 (1990).
[46] URL: `http://www.nndc.bnl.gov/ensdf/`.
[47] E. Runte et al., Nucl. Phys. A **441**, 237 (1985).
[48] E. R. Flynn, R. E. Brown, F. D. Correll, D. L. Hanson, and R. A. Hardekopf, Phys. Rev. Lett. **42**, 626 (1979).
[49] S. Cochavi and W. R. Kane, Phys. Rev. C **6**, 1650 (1972).
[50] M. Block et al., Phys. Rev. Lett. **100**, 132501 (2008).
[51] M. Block et al., Phys. Rev. Lett. **101**, 059901(E) (2008), erratum of Ref. [50].
[52] J. M. Daugas et al., AIP Conf. Proc. **831**, 427 (2006).
[53] S. Czajkowski et al., Z. Phys. A **348**, 267 (1994).
[54] D. Radford, Nucl. Instr. Met. Phys. Res. A **361**, 297 (1995).
[55] P. Bakoyeorgos, T. Paradellis, and P. A. Assimakopoulos, Phys. Rev. C **25**, 2947 (1982).
[56] E. K. Warburton, J. W. Olness, A. M. Nathan, J. J. Kolata, and J. B. McGrory, Phys. Rev. C **16**, 1027 (1977).
[57] M. Sawicka et al., Eur. Phys. J. A **16**, 51 (2003).
[58] O. Ivanov, Ph.D. thesis, Katholieke Universiteit Leuven (2007).
[59] K. W. C. Stewart, B. Castel, and B. P. Singh, Phys. Rev. C **4**, 2131 (1971).
[60] K. Heyde, P. Van Isacker, M. Waroquier, J. L. Wood, and R. A. Meyer, Phys. Rep. **102**, 291 (1983).